Chin. J. Astron. Astrophys. Vol. 2 (2002), No. 3, 266–276
(http://www.chjaa.org or http://chjaa.bao.ac.cn)

Chinese Journal of
Astronomy and
Astrophysics

Magnetic Field Strengths and Structures from Radio Observations of Solar Active Regions

Chang-Xi Zhang[1,2] ⋆, G. B. Gelfreikh[3] and Jing-Xiu Wang[4]

[1] Department of Astronomy, Peking University, Beijing 100871
[2] Chinese Academy of Science-Peking University Joint Beijing Astrophysics center, Beijing 100871
[3] Pulkovo Astronomical Observatory, 196140 St. Petersburg, Russia
[4] National Astronomical Observatories, Chinese Academy of Sciences, Beijing 100012

Received 2001 December 25; accepted 2002 March 28

Abstract Radio observations of some active regions (ARs) obtained with the Nobeyama radioheliograph at λ=1.76 cm are used for estimating the magnetic field strength in the upper chromosphere, based on thermal bremsstrahlung. The results are compared with the magnetic field strength in the photosphere from observations with the Solar Magnetic Field Telescope (SMFT) at Huairou Solar Observing Station of Beijing Astronomical Observatory. The difference in the magnetic field strength between the two layers seems reasonable. The solar radio maps of active regions obtained with the Nobeyama radioheliograph, both in total intensity (I-map) and in circular polarizations (V-map), are compared with the optical magnetograms obtained with the SMFT. The comparison between the radio map in circular polarization and the longitudinal photospheric magnetogram of a plage region suggests that the radio map in circular polarization is a kind of magnetogram of the upper chromosphere. The comparison of the radio map in total intensity with the photospheric vector magnetogram of an AR shows that the radio map in total intensity gives indications of magnetic loops in the corona, thus we have a method of defining the coronal magnetic structure from the radio I-maps at λ=1.76 cm. Analysing the I-maps, we identified three components: (a) a compact bright source; (b) a narrow elongated structure connecting two main magnetic islands of opposite polarities (observed in both the optical and radio magnetograms); (c) a wide, diffuse, weak component that corresponds to a wide structure in the solar active region which shows in most cases an S or a reversed S contour, which is probably due to the differential rotation of the Sun. The last two components suggest coronal loops on different spatial scales above the neutral line of the longitudinal photospheric magnetic field.

Key words: Sun: active regions — Sun: magnetic fields — Sun: optical observation — Sun: radio observation

⋆ E-mail: zhcx@vega.bac.pku.edu.cn

1 INTRODUCTION

The dominating role of magnetic field in the energy supply and structuring of the solar plasma is well known today. However, the measurement of the magnetic field in the chromosphere and corona, where most of the energy release occur, is beyond the capabilities of optical astronomy. Nowadays our study of the coronal magnetic field is usually based on extrapolation of the photospheric magnetic field or on the structure of high-temperature plasma found from space observations in X-rays or EUV lines.

Direct measurement of the magnetic field in the chromosphere and corona comes from radio observations, but not all of the radio observations are capable of providing the distribution of the field strength and its direction in 2D or 3D space (Alissandrakis 1999; Gelfreikh 1994; Gelfreikh 1996; Gelfreikh 1998; Grebinskij et al. 1999; Ryabov et al. 1999; Alissandrakis et al. 1980; Lee et al. 1993). All the methods are based on the theory of generation and propagation of radio emission in cosmic plasma. Some of them need high 2D spatial resolution and high polarization sensitivity with good wavelength coverage. This puts serious limits to the use of radio astronomical methods in modern solar physics, and this limitation can be partially overcome in collaborative programs involving several instruments with different capabilities.

Taking gyroresonance as the dominant emission mechanism, many studies have been done to calculate the magnetic field in the higher chromosphere, the lower corona and the transition region. Alissandrakis et al. (1980) calculated 2-dimensional maps of total intensity and circular polarization of a sunspot region at 6 cm using a simple model and observations of the longitudinal photospheric magnetic field. The good agreement between the calculations and the observations of the same sunspot region at 6 cm shows that the 6 cm radiation is predominantly due to the gyroresonace process at the second and third harmonics of the gyrofrequency and that the magnetic field in the the chromosphere-corona transition region is 600–900 G. Lee et al. (1993) first took steps to determine the harmonic number by combining high-frequency resolution observation of the gyroresonance brightness temperature spectrum and magnetogram observations of a round spot located near the disk center; they obtained an empirical determination of the coronal magnetic field by using the property that the microwave emission is only observable above a certain frequency given by an integer-multiple of the gyrofrequency. By using the spectral and polarization observations of the local sources of the S-component of solar radio emission made with RATAN-600 in the wavelength range 2.0–4.0 cm with high resolution, Akhmedov (1982) measured the maximum of the magnetic field of the corresponding sunspots at the height of the chromosphere-corona transition region. Their method was based on determining the short wavelength limit of gyroresonance emission of the local source and relating it to the third harmonic of gyrofrequency.

Ryabov et al. (1999), based on the radio mapping (in both Stokes I and V) of an active region undergoing circular polarization inversion, calculated a magnetogram of the coronal magnetic field. Their method focused on the quasi-transverse propagation of radiation and was not concerned with the details of emission mechanism.

In the present paper, we make estimates of the magnetic field strength above two active regions (a sunspot region and a plage region) in the upper chromosphere, on the basis of thermal bremmstrahlung. We also compare the solar radio maps of the active regions obtained with the Nobeyama radioheliograph at λ=1.76 cm, both in total intensity (I-map) and in circular polarizations (V-map) with the optical magnetograms. These comparisons show that the solar radio maps—both the I-map and the V-map—give some information on the magnetic field in the upper chromosphere and lower corona.

2 OBSERVATIONS

2.1 Optical Data

The optical magnetograms for the longitudinal and transverse magnetic fields in the photosphere (Fe I line 5324.2 Å) used in this study were obtained with the Solar Magnetic Field Telescope (SMFT) at the Huairou Solar Observing Station (HSOS) (Ai & Hu 1986). This vector magnetograph has a tunable birefringent filter, which can tune its working passband to the photospheric line Fe I λ5324.19Å, or to the chromospheric line H_β. For the photospheric observations, the passband is tuned to –0.075 Å off-band to measure the longitudinal component of the field, and to the line center to measure the transverse component, for maximum sensitivity. In the measurement of the magnetic fields in solar active regions, an integration of 255 frames and a smoothing over 4×3 pixels are usually taken for an increased signal-to-noise ratio. The magnetograms processed by the smooth averaging have a spatial resolution of about $2''$. The calibration for magnetic fields has been developed by Ai et al. (1982).

Many factors may affect the quantitative measurement of vector magnetic field. The limitation and reliability of the HSOS database were discussed by Wang et al. (1996). They argued that for the SMFT such factors as Zeeman saturation, Doppler shift, Faraday rotation and cross talk are insignificant. In the sunspot umbra area, however, contamination by stray light is serious. Nevertheless the observed line-of-sight flux density is reliable, and the azimuth of the transverse field is reasonably good when the region is close to the disk center.

2.2 Nobeyama Radio Maps

Nobeyama radioheliograph observations at $\lambda = 1.76\,$cm were used to restore the structure of the magnetic fields in the active regions. The V-maps (in circularly polarized component) were used to find the longitudinal component of the field, while the I-maps (in total intensity) were considered as source of information on the structures (loops) in the plasma of the solar atmosphere.

In most cases we used a routine, 10-seconds-averaging procedure, resulting in a sensitivity of about 1%, corresponding to a magnetogram sensitivity of about 100 G. To acquire better results for some of the data we also adopted averaging the images over 10-minute intervals, then the sensitivity is an order of magnitude better. The spatial resolution of the radio map is $10'' - 15''$. More details on the Nobeyama radioheliograph were given by Nakajima et al. (1994).

3 ESTIMATES OF MAGNETIC FIELD STRENGTHS

3.1 The Basic Equations

Bogod and Gelfreikh (1980) developed a method of measuring the magnetic fields in the solar corona and the chromosphere, on the basis of thermal bremmstrahlung. In their theory the absorption coefficient κ is found from the equation,

$$\kappa^{r,l} = \frac{\zeta \cdot N_e^2}{T^{3/2} \cdot (f \mp f_B \cdot \cos(\alpha))^2}. \quad (1)$$

Here the coefficient $\zeta \approx 0.15$, Ne is electron density, T — temperature, f — frequency of the radio wave, f_B — electron gyrofrequency, α — the angle between the magnetic vector and the line of sight. The sign of the polarization depends on the direction of the magnetic field and the mode: for x-mode it is right-handed (r) when the magnetic field is directed toward the observer (N — polarity) and it is left-handed for the opposite direction of the longitudinal component of the magnetic field. For the ordinary mode we have the opposite sign of circularly polarized component. In the formula above '+' refer to the ordinary mode in the case of positive magnetic field (directed toward the observer). Naturally, the absorption is higher for the extraordinary (x-) mode.

The optical depth is determined by the expression

$$\tau^{r,l} = \int \kappa^{r,l} \mathrm{d}l\,. \tag{2}$$

The brightness temperature T_{b}^{I} in the intensity (I-channel) is defined as

$$T_{\mathrm{b}}^{I} \equiv \frac{T_{\mathrm{b}}^{r} + T_{\mathrm{b}}^{l}}{2}, \tag{3}$$

and in the circular polarization (V-channel) as

$$T_{\mathrm{b}}^{V} \equiv \frac{T_{\mathrm{b}}^{r} - T_{\mathrm{b}}^{l}}{2}. \tag{4}$$

So, the difference in brightness temperature between the two polarized waves is $\Delta T_{\mathrm{b}} = T_{\mathrm{b}}^{r} - T_{\mathrm{b}}^{l} = 2 \times T_{\mathrm{b}}^{V}$.

The degree of circular polarization is defined as

$$P \equiv \frac{T_{\mathrm{b}}^{r} - T_{\mathrm{b}}^{l}}{T_{\mathrm{b}}^{r} + T_{\mathrm{b}}^{l}}. \tag{5}$$

The solution of the equations of radiative transfer for a weak magnetic field ($f_B \ll f$) for the percentage polarization can be written as

$$P = n \cdot \frac{f_B}{f} \cdot \cos(\alpha). \tag{6}$$

It follows that the longitudinal component of the magnetic field can be found from the observations as

$$B_l = \frac{107}{\lambda \cdot n} \cdot P\%. \tag{7}$$

In the formula for the longitudinal magnetic field $B_l = B \cdot \cos(\alpha)$ (Gauss), the sign of circular polarization should be included in the percentage polarization $P\%$, and the wavelength λ should be in cm.

For the Nobeyama radioheliograph, the observations show that the increase in brightness in solar active regions at $\lambda = 1.76\,\mathrm{cm}$ is usually rather small. So it seems reasonable to assume $n = 0.61$ (in reasonable agreement with observational data of the quiet sun). Then we obtain the formula to estimate the magnetic field strength from the Nobeyama radio maps for the percentage polarization

$$B_l \approx 100 \cdot P\%. \tag{8}$$

As the increase in brightness temperature in the plage/faculae-associated components of active regions is usually rather small ($\Delta T_{\rm b} \leq 50\%$), using the values ($T_{\rm b}^{I} \approx 10^4$ K and $n \approx 0.6$), typical of the quiet sun radio emission may give a reasonable approximation. This leads us to another simple formula for the chromospheric magnetic field in an active region

$$B_l \approx T_{\rm b}^{V} . \tag{9}$$

3.2 Estimating the Field Strengths

Above sunspots, we can usually observe the bright microwave radio emission excited by the thermal cyclotron (gyroresonance) mechanism. Electrons of the lower corona and chromosphere-corona transition region (CCTR) produce this type of sunspot-associated sources. These are usually easy to identify due to high brightness temperatures ($T_{\rm b} \geq 10^5$ K) and high degrees of polarization ($P \geq 50\%$). The strength of the magnetic field in the hot region of the solar atmosphere above sunspots is found from the condition of the generation of the radio emission at the third harmonic of the gyro frequency (Akhmedov et al. 1982)

$$B = \frac{3570}{\lambda}. \tag{10}$$

In the case of Nobeyama data, however, we need $B \geq 2000$ G in the lower corona to generate this component. This is a rather stringent condition. So, bright and highly polarized sources are observed only in a small percentage of sunspots. However, magnetic fields of sunspots from the Nobeyama radio heliograms in the absence of the cyclotron emission at λ=1.76 cm can be found from an analysis of polarized thermal bremsstrahlung emission. The estimate of the strength of the magnetic field in the sunspot AR (N20W05) on 1999 July 24 is given in Table 1.

When examining the magnetic fields in the flocculi regions, the noise level is always an essential factor limiting the sensitivity of the method. In the case of the usually used averaging time of 10 seconds the sensitivity (root mean square value) is proved to be equal to 70 K in the V-channel. Equation (9) suggests a sensitivity in the magnetic field of $\Delta B_l \approx 70$ G. For improving the sensitivity of radio magnetograms we use the radio maps averaged over 10-minute time scales (see Gelfreikh. 1999), resulting in $\Delta B_l \approx 9$ G. An estimate of the magnitude of magnetic field in the flocculus AR (N10, W2) on 1995 June 9 is given in Table 2.

Table 1 Maximum Magnetic Field Strengths in the Sunspot of 1999 July 24 (found by Different Methods)

Source	N-polarity	S-polarity	Method
Optical (Huairou)	2640	2340	Zeeman splitting of Fe 5324Å
Radio (P%)	1530	1490	Thermal bremsstrahlung

Table 2 Maximum Magnetic Field Strengths of the AR (N10, W2) on 1995 June 09

Method	N-polarity	S-polarity
Optical	740	660
Radio ($T_{\rm b}^{V}$)	430	400
Radio (P%)	280	280

4 COMPARISON BETWEEN THE RADIO MAP IN CIRCULAR POLARIZATION AND THE PHOTOSPHERIC LONGITUDINAL MAGNETOGRAM

When we deal with radio map of a plage in circular polarization from the Nobeyama radioheliograph, the microwave at 1.76 cm is usually generated by the thermal bremsstrahlung mechanism. It provides essential information on the magnetic field in the upper chromosphere (Gelfreikh & Shibasaki 1999).

Comparison between the optical and radio magnetography is illustrated in Figure 1 in which an optical magnetogram of the longitudinal component of the field found in Fe I line λ5324.19 Å is shown. As the spatial resolution here is about 2 arcsec, an order of magnitude higher than the Nobeyama radioheliograph data, we have averaged the optical data with a weighting function representing the beam of the Nobeyama radioheliograph (10–15 arcsec halfwidth). The radio magnetogram is shown here by contour lines of radio brightness in the channel of the circular polarization.

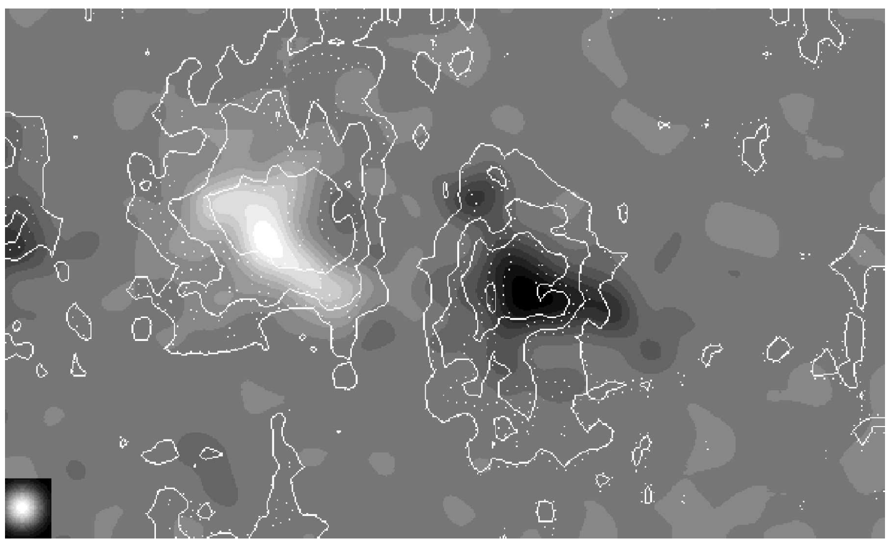

Fig. 1 Optical magnetograms of the solar AR (N10, W2) obtained on 1995 June 9 at 03:47 UT in the Fe I 5324.19 line. The magnetogram is averaged with the weight function representing the beam width of the Nobeyama radio heliograph. The solid (dotted) contours represent the levels of the circularly polarized emission or the V-map (percentage of polarization or the P-map) at λ=1.76 cm.

The result of this comparison leads us to a significant conclusion: the optical and radio methods give the same general structure of the magnetic field in a plage region of the solar atmosphere at spatial scales exceeding 10 arcsec. The radio data refer to the upper levels of the chromosphere while optical magnetograms refer to the photosphere. For the magnetic fields averaged over scales of about 10 thousand km we would not expect great differences in these two different layers. Differences could arise, however, from possible impact of some radio emission (both in V and I channels) from the corona where the scale of the radio source and the corresponding magnetic field could be orders of magnitude different. The good agreement in structure between the optical and radio magnetograms shows that this effect is not important in the present case.

From two types of radio magnetography (the V-maps drawn solid and the P-maps drawn dotted) in Figure 1 we find that the main features in both cases are quite similar. However, in the percentage radio map the agreement looks even more convincing.

5 COMPARISONS OF RADIO MAPS IN TOTAL INTENSITY WITH VECTOR MAGNETOGRAMS AND THE EXTRAPOLATED CORONAL FIELDS

Figures 2 and 3 illustrate a typical situation we found when comparing optical longitudinal magnetograms with intensity radio maps of an active region near the central meridian of the Sun. The V-map (and P-map) is a longitudinal magnetogram and implies a dipole magnetic structure in the region. The I-map looks quite different and has maximum intensity near the position of the neutral line of the longitudinal magnetic field (B_l=0). The maximum above the neutral line (NL) is typically rather narrow. The observed emission structure that connects the two magnetic polarities suggests to us a magnetic loop with its feet at the chromosphere/photosphere level. This is supported by the observation of some active regions near the limb where we can see the maximum of radio emission displaced from the NL of the longitudinal magnetic field at lower level (see Gelfreikh 1999).

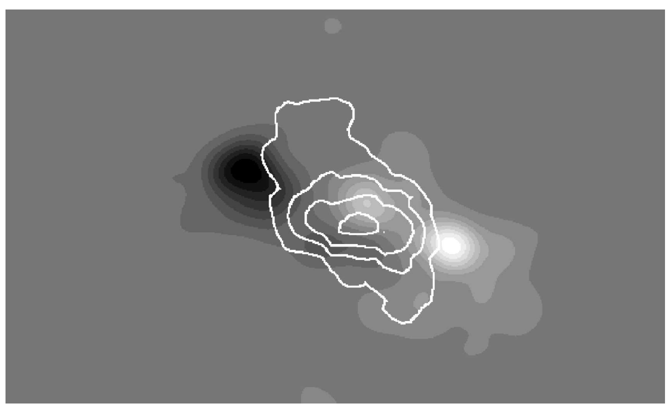

Fig. 2 Comparison of the radio I-map (contour lines) and optical magnetogram of the longitudinal component (grey-scale) of AR (N25, W10) on 1999 June 15.

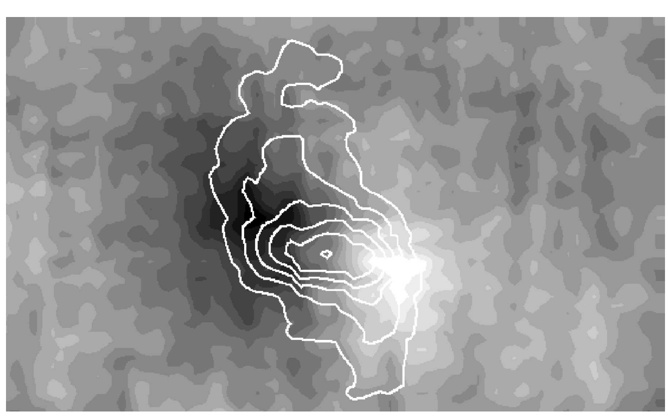

Fig. 3 Comparison of radio I-map and V-map at λ=1.76 cm of AR (N25, W10) on 1999 June 15. Contours of I-map are superimposed on the grey-scale map of polarization.

We should pay attention to the wide diffuse and weak S-like structure on the I-map elongated in N-S direction in Figures 2 and 3. It is shown that this component of the source also follows the general structure of the NL of the photospheric longitudinal magnetic field. We suppose that it is related to a system of loops at smaller heights. The S-like structure of the source in this case must be due to the effect of the differential solar rotation (higher angular velocities at lower heliographic latitudes).

To check our supposition we have compared the I-map with the structure of the extrapolated magnetic field in the corona and the optical vector magnetogram. The numerical method for this extrapolation was proposed by Yan and Sakurai (2000), and the method of data reduction for the vector magnetograms was suggested by Wang, Yan and Sakurai (2001). The vector magnetogram of the AR on 1999 June 15 is shown in Figure 4. The general alignment of the photospheric transverse field near the NL resembles the shape of the S-like structure in the radio I-map shown in Figures 2 and 3. In Figure 5 we show the structure of the computed magnetic field of the corona in the force-free approximation. The S-like structure on the radio map here appears to be in agreement with the suggestion of its being connected to the coronal magnetic field structure.

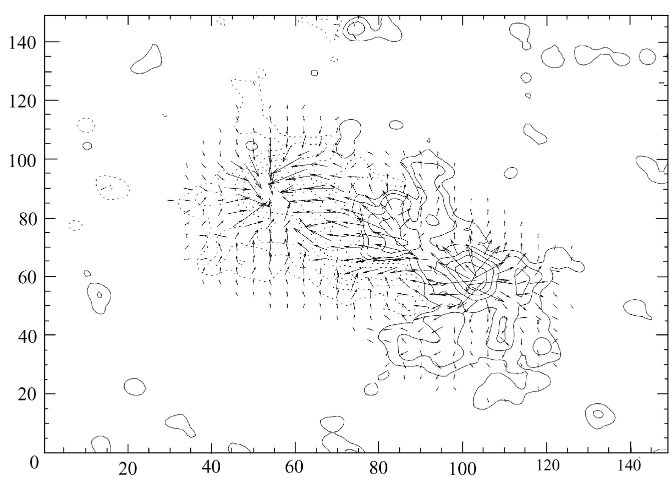

Fig. 4 Photospheric vector magnetic field of AR (N25, W10) on 1999 June 15.

Within the diffuse s-like structure there is a narrow and elongated brighter structure, which links two main islands of magnetic fields of different polarity. It seems to represent the magnetic loops that connect two main patches of different magnetic polarities. Within the narrow structure of the I-map, there is a small patch of total intensity of radio emission and it has the maximum strength. This case seems related to the small-scale complex structure of magnetic fields.

One more example is used to illustrate a different case of the radio maps of an AR (1992 October 25) at the wavelength λ=1.76 cm. This radio magnetogram is presented in Figure 6, the I-map (total intensity) is shown by contour lines and the P-map (percentage of polarization) is shown by gray map.

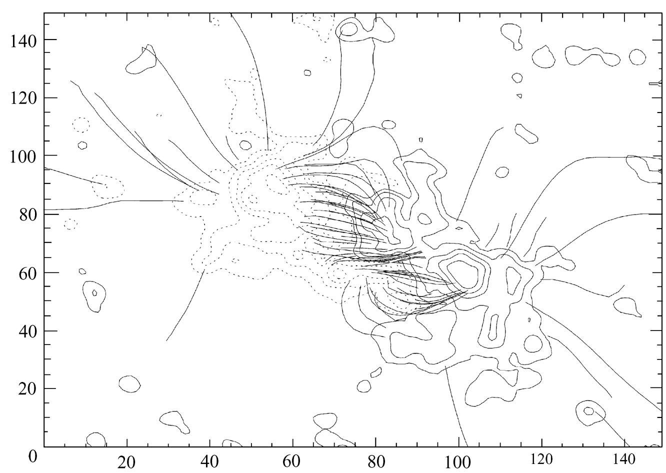

Fig. 5 Structure of the lower magnetic field lines in an AR (N25, W10) observed on 1999 June 15 found by extrapolation of the vector magnetograms of the photospheric field under the force-free approximation.

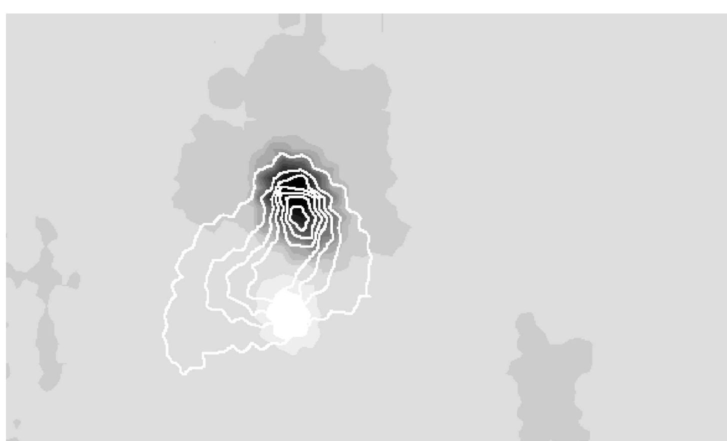

Fig. 6 Radio percentage polarization(P-map) observed on 1992 October 25 in AR (S25, E08) (grey-scale map) and the contours for I-maps. The maximum brightness is $T_{\rm b} = 125 \times 10^3$.

In this case not only thermal bremsstrahlung but also the thermal cyclotron emission is present. It is evidenced by the high temperature ($T_{\rm b} = 125 \times 10^3\,$K) and highly polarized ($P\% = 64$) compact source above the local patch of stronger field of the sunspot umbra. On the other hand we can follow all the main features of the ARs with developed dipole magnetic structures: the narrow "loop" connecting two islands of stronger magnetic fields of different polarities and the other, more diffuse component following the NL of the AR. In this condition the axis of the magnetic dipole follows mostly NS direction. Nevertheless, the effect of differential rotation mentioned above can be clearly seen: the region being in the southern hemisphere, the effect results in a reversed S-like structure.

6 CONCLUSIONS AND DISCUSSION

The most important advantage of the radio magnetograms based on the Nobeyama radioheliograph observations is due to their unprecedented full bank of data, observed at intervals of 10 seconds and over 8 hours every day since July 1992. The main limitations of the method arise from the low spatial resolution of about 10 arcseconds of the radio maps and some uncertainties in obtaining the magnetic field strength. The latter is mostly due to the absence of spectral analysis on this instrument. The resolution limitation simply means that the data are adequate mostly for studying magnetic structures more than 10 000 km on the solar surface.

A remaining problem is the identification of the level of the solar atmosphere (chromosphere/corona) where we derived the magnetic fields from the Nobeyama radio V-maps. This point was already discussed in some previous papers (Gelfreikh 1999; Grebinskij et al. 2000) but it seems that more additional studies are needed.

Taking the foregoing factors into account, we have obtained a reasonable result of the magnitude of the magnetic fields in the upper solar chromosphere. The map comparisons show that the V-map and the maps for percentage polarization (P-maps) give a good display of the distribution of the longitudinal magnetic field, mostly at the level of the upper solar chromosphere, indicating structures with dimensions above 10 000 km.

A comparative analysis of the I-maps with both the optical magnetograms and radio V-maps indicates that we can acquire two pieces of information of coronal magnetic loops from the structure of the radio I-map: one structure reflects the loops connecting the two main parts of stronger longitudinal magnetic fields, another reflects the larger scale loop system connecting most parts of negative and positive polarities, elongated along the neutral line, and with an S or a reversed S pattern (Figures 2, 3, and 6). Its evolution is correlated with the effect of the differential solar rotation. The comparison of the optical vector magnetogram with the field in the corona confirms that the enhanced emission seen in the I maps of ARs originates in the coronal loop. The I-map also shows a smaller patch of the brightest part. The compact patch lies either at the neutral line or at one magnetic island.

From our study, the following conclusions are drawn:

1. On the basis of thermal bremmstrahlung, we can obtain rough and reasonable estimates of the magnitude of magnetic field in the upper chromosphere, i.e., our approximate formula works well for some proper active regions.

2. The magnetic field structure from the radio polarization maps is in good agreement with that of the longitudinal magnetograms of the photosphere.

3. From an analysis of the AR I-maps, and from their comparison with the corresponding magnetograms, we can identify three components related to the different elements of the magnetic field of the AR (see Figure 2).

(a) One component is the compact bright source either above the position of the NL of the longitudinal magnetic field or above the strongest part of one polarity. The typical brightness temperature of this component is found to be in the range 30×10^3 K to 100×10^3 K. In some cases it is found connected with the local small-scale structures of the photospheric field (not seen on radio magnetograms).

(b) The narrow elongated structure, connecting the two main magnetic islands of different polarities (observed in both the optical and radio magnetograms), may indicate the presence of magnetic loops in the solar corona.

(c) The wide diffuse and weak component ($\Delta T_{\rm b}^{I} \approx 3 \times 10^{3}$) corresponds to a wide structure of the AR and shows in most cases the S or reversed S contour which is probably due to the differential rotation of the sun (Figures 2 and 6).

In our study we tend to work with ARs near the central meridian, to avoid the effect of inversion of the sign of polarization and effect of projection. These also contain important information on the 3D structure and other parameters of the magnetic field of solar ARs. They need, however, further and more detailed studies.

All the results above show that a proper use of the regular Nobeyama radio heliograph observations provides a new way to study in detail the time evolution of solar activity on scales from minutes to years. More effective studies of the solar magnetic field in both the chromosphere and corona based on radio observations, need instruments with similar time and spatial resolutions to Nobeyama, additionally with good spectral analysis.

Acknowledgements We thank Prof. Aihua Zhou and Huaning Wang for their help. Thanks are given to all members of Huairou solar observing station of BAO for supplying the optical data.

References

Ai G., Hu, Y., 1986, Publ. Beijing Astron, 8, 1

Ai G., Li W., Zhang H., 1982, Chinese Astronomy and Astrophysics, 6, 129

Akhmedov Sh. B., Gelfreikh G. B., Bogod V. M., Korzhavin A. N., 1982, Solar Phys., 79, 41

Alissandrakis C. E., 1999, NRO Report, 479, 53

Alissandrakis C. E., Kundu M. R., Lantos P., 1980, A&A, 82, 30

Bogod V. M., Gelfreikh G. B., 1980, Solar Phys., 67, 29

Gelfreikh G. B., 1994, In: V. Rusin, P. Heizel, J.-C. Vial, eds., IAU Colloquium 144, Solar Coronal Structures, p.21

Gelfreikh G. B., 1996, In: A. R. Taylor, J. M. Paredes, eds., ASP Conf. Ser. Vol. 93, Radio Emission from the Stars and the Sun, p.415

Gelfreikh G. B., 1998, In: C. E. Alissandrakis, B. Schmieder, eds., ASP Conf. Ser. Vol. 155, Second Advances in Solar Physics Euroconference: Three-Dimensional Structure of Soalr Active Regions, p.110

Gelfreikh G. B., 1999, NRO Report, 179, 41

Gelfreikh G. B., Shibasaki K., 1999, In: A. Wilson, ed., Proc. 9th European Meeting on Solar Physics, Magnetic Field and Solar Process, p.1339

Grebinskij A., Bogod V., Gelfreikh G. B., Urpo S., Pohjolinen S., Shibasaki K., 2000, A&AS, 144, 169

Grebinskij A., Shibasaki K., Zhang H., 1999, NRO Report, 479, 59

Lee J. W., Hurford G. J., Dary D. E., 1993, Solar Phys., 144, 45

Nakajima H., Nishio M., Enome S., Shibasaki K., Takano T., Hanaoka Y., Torii C., Sekiguchi H., Bushimata T., Kawashima S., Shinohara N., Irimajiri Y., Koshiishi H., Kosugi T., Shiomi Y., Sawa M., Kai K., 1994, Proc IEEE, 82, 705

Ryabov B. I., Pilyeva N. A., Alissandrakis K. E., Shibasaki K., Bogod V. M., Garaimov V. I., Gelfreikh G.B., 1999, Solar Phys., 185, 157

Wang H. N., Yan Y., Sakurai T., 2001, Solar Phys., 201, 323

Wang J., Shi Z., Lu Y., Wang H., 1996, ApJ, 456, 861

Yan Y., Sakurai T., 2000, Solar Phys., 195, 89